



# An autophagy-inducing stapled peptide promotes c-MET degradation and overrides adaptive resistance to sorafenib in c-MET<sup>+</sup> hepatocellular carcinoma

Shan Gao<sup>a</sup>, Na Li<sup>b</sup>, Xiaozhe Zhang<sup>a</sup>, Jingyi Chen<sup>a</sup>, Ben C.B. Ko<sup>a</sup>, Yanxiang Zhao<sup>a,b,\*</sup>

<sup>a</sup> Department of Applied Biology and Chemical Technology, State Key Laboratory of Chemical Biology and Drug Discovery, The Hong Kong Polytechnic University, Hung Hom, Kowloon, Hong Kong, 999077, PR China

<sup>b</sup> The Hong Kong Polytechnic University Shenzhen Research Institute, Shenzhen, 518057, PR China

## ARTICLE INFO

### Keywords:

HCC  
EGFR  
c-MET  
Autophagy  
Endolysosomal degradation

## ABSTRACT

**Background:** Hepatocellular carcinoma (HCC) accounts for approximately 90% of primary liver cancer cases and ranks as the second leading cause of cancer related death. Multiple receptor tyrosine kinases such as EGFR, FGFR and c-MET have been shown to drive tumorigenesis and progression of HCC. However, tyrosine kinase inhibitors (TKIs) that target these kinases, including the FDA-approved sorafenib, only offer limited clinical success. Resistance to sorafenib and other TKIs also readily emerge in HCC patients, further limiting the usage of these drugs. Novel therapeutic strategies are needed to address the urgent unmet medical need for HCC patients.

**Results:** Autophagy is an evolutionally conserved lysosome-dependent degradation process that is also functionally implicated in HCC. We previously developed an autophagy-inducing stapled peptide (Tat-SP4) that induced autophagy and endolysosomal degradation of EGFR in lung cancer and breast cancer cells. Here we present data to show that Tat-SP4 also induced significant autophagic response in multiple HCC cell lines and promoted the endolysosomal degradation of c-MET to attenuate its downstream signaling activities although it didn't affect the intrinsically fast turnover of EGFR. Tat-SP4 also overrode adaptive resistance to sorafenib in c-MET<sup>+</sup> HCC cells but employed the distinct mechanism of inducing non-apoptotic cell death.

**Conclusion:** With its distinct mechanism of promoting autophagy and endolysosomal degradation of c-MET, Tat-SP4 may serve as a novel therapeutic agent that complement and synergize with sorafenib to enhance its clinical efficacy in HCC patients.

## 1. Introduction

Hepatocellular carcinoma (HCC) accounts for approximately 90% of primary liver cancer cases. Globally it is ranked as the seventh most common cancer and the second leading cause of cancer death with 905,677 newly diagnosed cases and 830,180 deaths in 2020 [1]. HCC is particularly prevalent in a few geographical regions such as eastern and south-eastern Asia that account for more than 50% of worldwide new cases and deaths. The alarmingly high incidence of HCC in these regions is tied to a group of environmental and lifestyle risk factors such as chronic hepatitis B viral infection, over-consumption of alcohol and exposure to aflatoxins [2,3].

Therapeutic options for HCC patients are rather limited. More than

half of HCC cases are diagnosed in advanced stage when curative therapies like surgical resection and radiofrequency ablation are not applicable [2,3]. With compromised liver function, aggressive systemic treatments such as chemotherapy and radiation therapy are often of limited use [2,3]. Transarterial chemoembolization (TACE) is frequently applied to patients with unresectable HCC as palliative therapy to temporarily block tumor growth although tumor progression almost always resumes [2,3].

Two types of targeted therapeutics have been approved for HCC treatment in recent years, including tyrosine kinase inhibitors (TKIs) such as sorafenib, lenvatinib, regorafenib and cabozantinib; and monoclonal antibodies (mAbs) bevacizumab and ramucirumab [2–9]. TKIs exert their anti-proliferative effect by blocking the intracellular

\* Corresponding author. Department of Applied Biology and Chemical Technology, State Key Laboratory of Chemical Biology and Drug Discovery, The Hong Kong Polytechnic University, Hung Hom, Kowloon, Hong Kong, 999077, PR China.

E-mail address: [yanxiang.zhao@polyu.edu.hk](mailto:yanxiang.zhao@polyu.edu.hk) (Y. Zhao).

<https://doi.org/10.1016/j.bbrep.2022.101412>

Received 12 October 2022; Received in revised form 11 December 2022; Accepted 13 December 2022

2405-5808/© 2022 The Authors. Published by Elsevier B.V. This is an open access article under the CC BY-NC-ND license (<http://creativecommons.org/licenses/by-nc-nd/4.0/>).

kinase activity of many abnormally activated growth factor receptors in HCC such as EGFR, VEGFR, FGFR, PDGFR and c-MET; while mAbs exert similar inhibitory effect at the extracellular side [2–9]. However, all these drugs showed limited clinical success with survival benefit of ~2–3 months only. Novel strategies to target these receptor tyrosine kinases are needed to overcome the formidable network of abnormally activated growth signaling pathways in HCC.

Autophagy is a lysosome-dependent process that degrades and recycles cytosolic content to maintain cellular homeostasis [10–12]. A hallmark feature of autophagy is the formation of autophagosomes, which are double-membraned vesicles that sequester cytosolic proteins and organelles as autophagic cargo and traffic through the endosomal membrane system for fusion with lysosomes [10–12]. As a major metabolic organ, liver relies on autophagy to fulfill important function such as clearance of misfolded proteins, selective organelle degradation

and sustaining energy metabolism and under nutrient stress [13]. On the other hand, autophagy is also implicated in several risk factors for HCC such as HBV replication, alcohol-induced steatosis and non-alcoholic fatty liver disease [13]. The exact role of autophagy in HCC is not fully understood and its potential as a novel anti-HCC strategy deserves to be explored.

In our previous studies, we have developed a series of autophagy-inducing peptides by targeting an essential autophagy protein Beclin 1 [14,15]. These peptides are 26-residue in length, with a cell-penetrating Tat sequence of YGRKKRRQRRR at the N-terminal and the Beclin 1-targeting segment at the C-terminal (Fig. 1A). A 13-carbon hydrocarbon staple is added to the C-terminal segment so that the designed peptides adopt the  $\alpha$ -helical structure for specific binding to the Beclin 1 coiled coil domain [14,15]. These peptides readily promoted Beclin 1-mediated processes including autophagy and endolysosomal degradation of

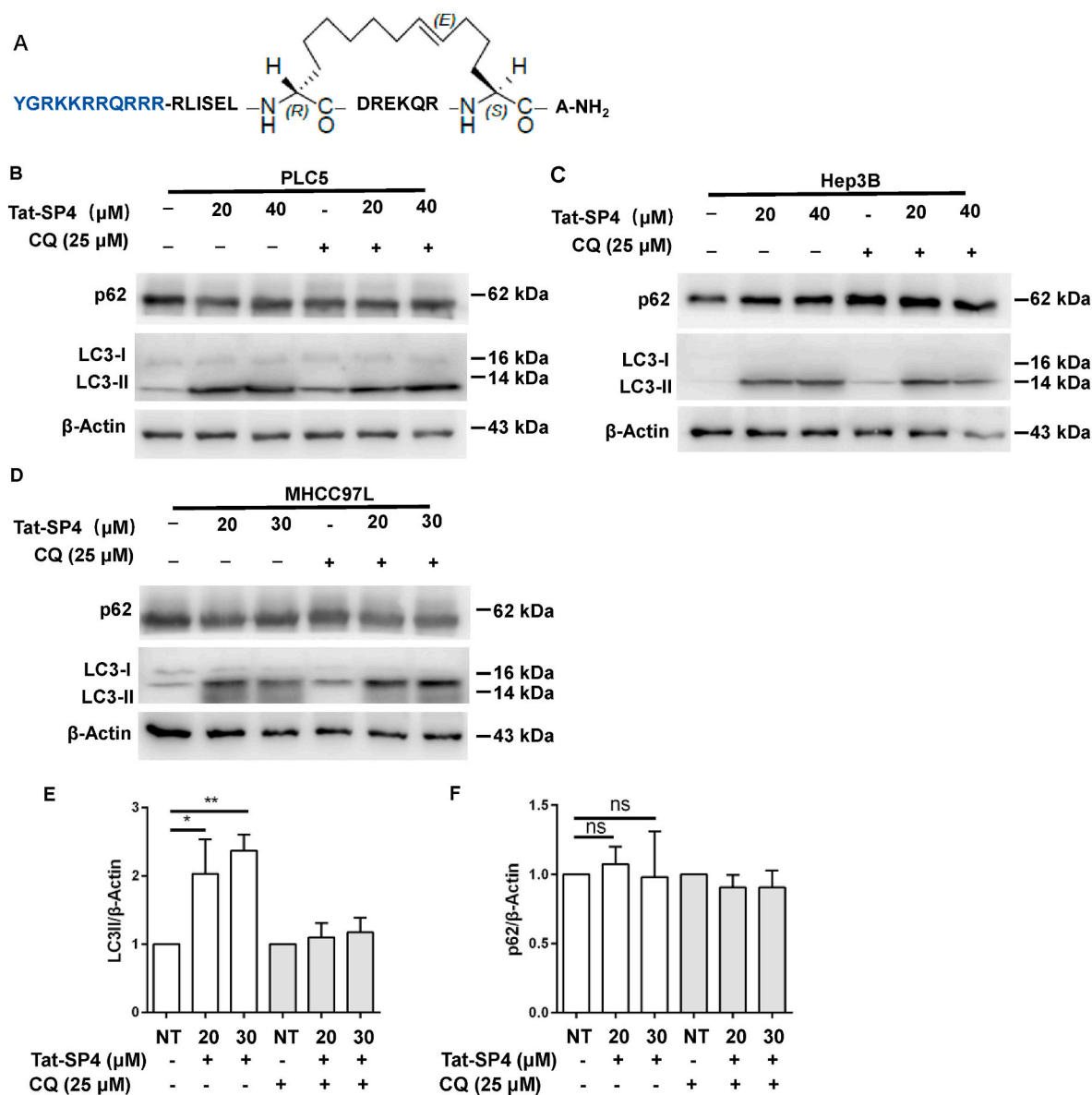


**Fig. 1.** Tat-SP4 induces significant autophagic response in different HCC cell lines. (A) The sequence and chemical structure of Beclin1-targeting stapled peptides binding to the coiled coil domain of Beclin1. The Tat sequence (colored in blue) is added to enable cell penetration. (B) Autophagy markers p62 and LC3-II were measured by Western blot in PLC/PRF/5 cells under basal condition and after treatment with 20 μM and 40 μM of Tat-SP4 for 3 h either with (+) or without (-) 25 μM CQ. (C & D) Similar western blots as (A), but for Hep3B (C) or MHCC97L (D) cells with concentrations of Tat-SP4 marked. (E & F) Quantification of LC3-II lipidation profile and p62 level from Western blot data in (B-D). The levels of LC3-II (E) or p62 (F) were normalized to the β-Actin level. Data are presented as mean ± SEM (n = 3). \*P < 0.05, \*\*P < 0.05, One-way ANOVA test. (For interpretation of the references to color in this figure legend, the reader is referred to the Web version of this article.)

EGFR in multiple cell lines including HEK293T, non-small-cell lung cancer cell lines (NSCLC) A549 and H1975, and the HER2<sup>+</sup> breast cancer cell line SKBR3 [14,15]. One lead peptide Tat-SP4 also showed anti-proliferative effect in SKBR3 by enhancing EGFR/HER2 degradation and inducing necrotic cell death [15].

Encouraged by this finding, we hypothesize that Tat-SP4 may show similar effect in HCC cells because of their dependence on autophagy and aberrant activation of the EGFR-mediated signaling network [2,3]. Here we report that Tat-SP4 induced varied autophagic response in HCC cell lines with diverse genetic background. In contrast to our previous observation in NSCLC and breast cancer cell lines, Tat-SP4 showed little effect on endolysosomal degradation of EGFR in HCC. Intriguingly, Tat-SP4 significantly enhanced the endolysosomal degradation of c-MET, a receptor tyrosine kinase similar to EGFR but is activated by hepatocyte growth factor (HGF) instead of EGF [16]. Tat-SP4 also attenuated the growth signals downstream of c-MET and overrode sorafenib resistance in c-MET<sup>+</sup> HCC cells. These data suggest that autophagy-inducing peptides may serve as novel therapeutic candidates that complement and synergize with sorafenib to enhance its clinical efficacy for HCC patients.

## 2. Materials and methods

**Reagents and antibodies.** Chloroquine (CQ; Sigma-Aldrich), Epidermal Growth Factor (EGF; Gibco), Hepatocyte growth factor (HGF; Invitrogen), sorafenib (Beyotime), EDTA-free protease inhibitor cocktail (Roche), Trypsin (Invitrogen), Trypan Blue (Gibco), anti- $\beta$ -Actin antibody (Santa Cruz), anti-LC3 antibody (Abnova), anti-p62 antibody (Abnova), anti-EGFR antibody (Santa Cruz), Rabbit anti-cMET antibody in WB (Cell Signaling Technology), mouse anti-cMet antibody in IF (Santa Cruz), anti-mouse IgG antibody conjugated with Alexa Fluor 555 (Invitrogen), anti-pMET antibody (Cell Signaling Technology), anti-Akt antibody (Cell Signaling Technology), anti-pAkt antibody (Cell Signaling Technology), anti-Mouse IgG-HRP (Sigma-Aldrich), anti-Rabbit IgG-HRP (Sigma-Aldrich), DAPI (Thermo fisher).

**Chemical synthesis of stapled peptides.** The Tat-SP4 stapled peptide was purchased from *GL Biochem (Shanghai) Ltd.* The synthesis process was the same as reported in our previous study [17]. Briefly, the peptide was synthesized by automated solid-phase method with olefin-containing amino acids incorporated at the designated positions. The hydrocarbon staple was formed on olefin-containing amino acids by ring-closing metathesis reaction using the Grubbs catalyst. Chemical structure and purity of the final product were characterized by HRMS and HPLC. Purity of each synthesized peptides is >95%. Stock solution of each obtained peptide was prepared by dissolving the sample in pure water to a concentration of 20 mM.

**Cell lines and cell culture.** The hepatocellular carcinoma (HCC) cell lines Hep3B were purchased from Stem Cell Bank, Chinese Academy of Sciences, Shang Hai, China. PLC5 were kindly gifted by Dr. Ben Ko's lab (The Hong Kong Polytechnic University). MHCC97L and MHCC97L-luc and sorafenib resistant MHCC97L-luc was kindly provided by Prof. Terence Lee's lab (The Hong Kong Polytechnic University). All cells were cultured in DMEM with 10% (v/v) FBS. Cells were grown in a humidified incubator with 5% CO<sub>2</sub> at 37 °C. Cell lines were regularly tested and verified to be mycoplasma negative by DAPI staining before and during experiments.

**Cell viability assay.** Cell viability was measured by trypan blue exclusion assay following the standard protocol provided by the manufacturer [18]. HCC cells were seeded into 96-well plates, with the starting cell number adjusted for each cell line to reach 80–90% final confluency after overnight incubation. Cells were treated with different concentrations of Tat-SP4 for 24 h or Sorafenib for 72 h. The number of viable cells were counted by the Z1 Particle Counter (Beckman Coulter). The IC<sub>50</sub> values were calculated after curve fitting using the concentration-response data sets. All experiments were repeated in triplicate and the mean values were calculated.

**5-day proliferation assay.** 5-day cell proliferation assay was performed to test the long-term anti-proliferation effect of Tat-SP4 using the same protocol of our previous study [18]. HCC cells were seeded into 24-well and the initial cell number was determined based on the optimal cell growth rate for each cell line. After overnight incubation, cells were treated with Tat-SP4 or Tat-SC4. Cells were cultured over a time span of five days and the number of viable cells calculated every 24 h by Trypan Blue exclusion assay.

**Immunoblot analysis.** Western blots were carried out following the standard protocols used in previous studies [19,20]. Specifically, whole cell lysates were extracted using Laemmli sample buffer (62.5 mM Tris-HCl, pH 6.8, 2% SDS, 25% glycerol, 5%  $\beta$ -mercaptoethanol) supplemented with EDTA-free protease inhibitor cocktail (Roche). Protein concentration was determined using a standard Bradford assay before immunoblotting. Protein samples were separated by SDS-PAGE gel, transferred to a PVDF membrane (Millipore, USA), and incubated with the primary antibodies and HRP-conjugated secondary antibodies. Protein bands were visualized using ECL reagents.  $\beta$ -Actin was used as the loading control.

**EGFR and c-MET degradation assay.** The endolysosomal degradation assay was carried out using the same protocol as our previous studies [14,15]. HCC cells in 6-well plate were washed with PBS two times and serum-starved overnight in DMEM medium. Endocytosis of EGFR and cMET were induced by treatment with 200 ng/mL of EGF, 100 ng/mL of HGF at 37 °C, respectively. Cells were collected at the indicated time points after EGF or HGF stimulation, lysed and subject to immunoblot analysis.

**Immunofluorescence analysis.** The immunofluorescence imaging assay was carried out using the same protocol as our previous study [14]. MHCC97L cells were plated on 18 mm  $\times$  18 mm glass slides in 6-well plate and washed with PBS twice before serum starvation for 12 h in DMEM medium. Then, cells were treated with either HGF (100 ng/mL) or Tat-SP4 (40  $\mu$ M) alone, as well as these two combined. Cells were harvested at the indicated time points after each stimulation. Cells were fixed with 4% paraformaldehyde and permeabilized with 1% Triton X-100 in PBS. Cells were blocked with 1% BSA and 0.2% Triton X-100 in PBS. Cells were then washed three times with PBS and incubated with the primary antibodies and Alexa Fluor 555-conjugated secondary antibodies. Slides were examined under a Leica invert confocal microscope (TCS-SP8-MP system). Images were taken with 63x oil immersion objective lens at room temperature and image acquisition was performed by LAS X software (Leica).

**Flow cytometry.** The degree of cellular apoptosis and necrosis were assessed by flow cytometry following the standard protocol provided by the manufacturer [21]. Briefly, MHCC-97L cells after the indicated peptide treatment were harvested by trypsin, labelled with Annexin V and PI (Invitrogen), loaded to the flow cytometer system (BD Accuri C6), and analyzed by BD Accuri C6 software. The cell populations could be distinguished by the staining of Annexin V/PI. Typically, cellular population in the lower left quadrant represents live cells (Annexin V<sup>-</sup>, PI<sup>-</sup>), the lower right quadrant represents early apoptotic cells (Annexin V<sup>+</sup>, PI<sup>-</sup>), the upper right quadrant represents late apoptotic cells (Annexin V<sup>+</sup>, PI<sup>+</sup>), and the upper left quadrant represents necrotic cells (Annexin V<sup>-</sup>, PI<sup>+</sup>) [19].

**Establishment of sorafenib-resistant MHCC97L-luc cells.** The sorafenib-resistant MHCC97L cell line was established in a previous study [22]. The wild-type MHCC97L cells was first modified to stably express the luciferase reporter gene (MHCC97L-luc). The sorafenib-resistant cells were established by subjecting the wild-type cells to continuous administration of gradually increasing concentrations of sorafenib up to 10  $\mu$ M. The same volume of dimethyl sulfoxide (DMSO) was added to the cells as mock controls during establishment of these resistant cells.

**Statistical analyses.** Results were presented as mean  $\pm$  SEM. Statistical significance was assessed by either two-tailed, unpaired Student's t-test or ordinary one-way ANOVA for multiple cohorts

(GraphPad Software). P values < 0.05 were considered statistically significant.

### 3. Results

#### 3.1. The autophagy-inducing stapled peptide Tat-SP4 triggers significant autophagic response in different HCC cell lines

HCC is an extremely heterogeneous disease involving numerous oncogenic pathways [23]. To reflect such heterogeneity, we picked three HCC cell lines including PLC/PRF/5, Hep3B and MHCC97L as they differ in terms of important HCC markers including hepatitis virus B (HBV), tumor suppressor p53 and proto-oncogene beta-catenin ( $\beta$ -cat). We treated these cell lines with Tat-SP4 at increasing concentrations of 20, 30 and 40  $\mu$ M as these dosages have been shown to be non-toxic to a panel of cell lines in our previous studies [14,15,18]. We then tracked two autophagy markers LC3 and p62 by western blots, as the increase of lipidated LC3 (termed LC3-II in contrast to the unlipidated LC3-I) and the decrease of p62 as a degraded autophagy receptor are reliable readout for cellular autophagic activity [10–12].

Our results reveal that Tat-SP4 induced significant autophagic response in all three HCC cell lines tested. In PLC/PRF/5 cells, the LC3-II level increased  $\sim$ 2–3 fold after Tat-SP4 treatment at 40  $\mu$ M while the p62 level remained largely unchanged (Fig. 1B, E & 1F). Addition of the autophagy inhibitor chloroquine (CQ) further potentiated the increase in LC3-II, thus confirming that Tat-SP4 induced autophagy instead of blocking it (Fig. 1B, E & 1F). Similar changes were observed in Hep3B and MHCC97L cells (Fig. 1C–F). Overall, Tat-SP4 induced significant autophagic response in HCC cell lines regardless of their genetic background.

#### 3.2. Tat-SP4 exerts little effect on the fast endolysosomal degradation of EGFR in HCC cell lines

Our previous studies showed that Tat-SP4 promoted endolysosomal degradation of EGFR in multiple cancer cell lines including NSCLC cell lines A549 and H1975 and breast cancer cell line SKBR3 [14,15]. To assess whether Tat-SP4 has similar effect in HCC cell lines, we tracked the level of EGFR after treatment by either the agonist EGF or Tat-SP4. Our data shows that 200 ng EGF triggered fast agonist-induced endolysosomal degradation of EGFR in PLC/PRF/5 cells, with the level of EGFR decreased by >50% at 2 h after EGF treatment and then further degraded by >80% after 4 h (Fig. 2A). However, treatment by Tat-SP4

alone showed no such effect with the level of EGFR steady even 4 h afterwards (Fig. 2A). Co-treatment by Tat-SP4 and EGF triggered fast EGFR degradation as well, but the kinetic profile was largely the same as stimulation by EGF alone (Fig. 2A). Similar effects were observed in Hep3B and MHCC97L cells, with EGF stimulation alone triggering even faster degradation of EGFR than in PLC/PRF/5 cells while Tat-SP4 showed no such effect (Fig. 2B and C). Immunofluorescence imaging of endogenous EGFR in MHCC97L cells further confirmed Tat-SP4 alone did not affect its abundance (Fig. 2D). In Summary, all three HCC cell lines showed fast EGFR turnover that was not further promoted by Tat-SP4 treatment.

#### 3.3. Tat-SP4 significantly enhances endolysosomal degradation of c-MET in HCC cells with c-MET over-expression

Intrigued by the finding that Tat-SP4 did not further promote the endogenous turnover rate of EGFR in HCC cells, we wondered if this outcome was specific for EGFR or applied to other cell surface receptors that also undergo agonist-induced endocytosis followed by subsequent endolysosomal degradation. Among the three HCC cells used in our study, MHCC97L stands out as the unique one because it over-expresses c-MET, a major growth factor receptor tyrosine kinase similar to EGFR but is activated by HGF instead of EGF [16]. In fact, c-MET is a proto-oncogene intimately involved in multiple cancer types and a major drug target for anti-cancer drug discovery [16].

Our data shows that c-MET in MHCC97L cells was detected as two bands of  $\sim$ 170 and  $\sim$ 140 kDa that represented the full-length precursor protein and the mature receptor respectively (Fig. 3A). Treatment by HGF did not induce noticeable endolysosomal degradation of either c-MET band in MHCC97L cells (Fig. 3A and B). To the contrary, the total amount of the 140-kDa mature c-MET and its phosphorylation level even increased noticeably in response to HGF stimulation (Fig. 3A and B). This profile is in distinct contrast to the fast turnover of EGFR we observed in the same cells and highlight the difference between these two receptors.

Tat-SP4 alone at 20  $\mu$ M triggered prompt and significant degradation of the 140-kDa mature c-MET, with  $\sim$ 30% degraded as soon as 30 min after treatment (Fig. 3A and B). Furthermore, Tat-SP4 alone also significantly reduced the phosphorylation level of the mature c-MET and its downstream target Akt (Fig. 3A). Co-treatment by Tat-SP4 and HGF led to c-MET degradation in the similar pattern as Tat-SP4 only (Fig. 3A and B). These data suggest the intriguing possibility that Tat-SP4 triggered rapid degradation of c-MET and attenuated the HGF/c-MET

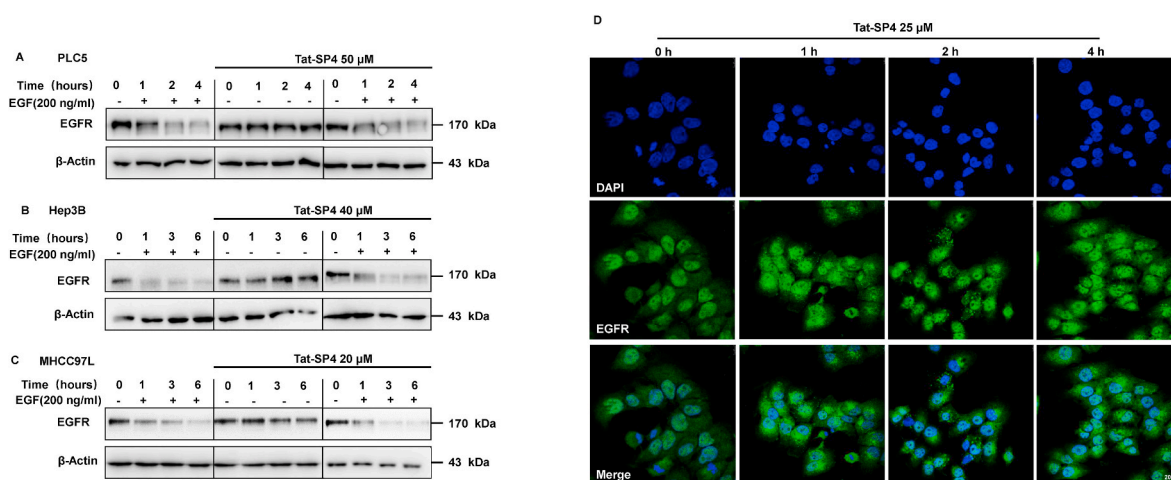


**Fig. 2.** Tat-SP4 shows little effect on the fast endolysosomal degradation of EGFR in HCC cells. The EGFR level in PLC5 (A), Hep3B (B), and MHCC97L (C) cell lysate was analyzed by Western blot at indicated time points after overnight serum-free starvation (–) and 200 ng/mL EGF treatment (+), Tat-SP4 (50, 40, 20  $\mu$ M) treatment, respectively. (D) Immunofluorescence imaging of EGFR in MHCC97L cells before (0 h) and after treatment with 25  $\mu$ M Tat-SP4 at indicated time points after overnight serum starvation. Cells were blocked and incubated with anti-mouse Alexa Fluor secondary antibodies.



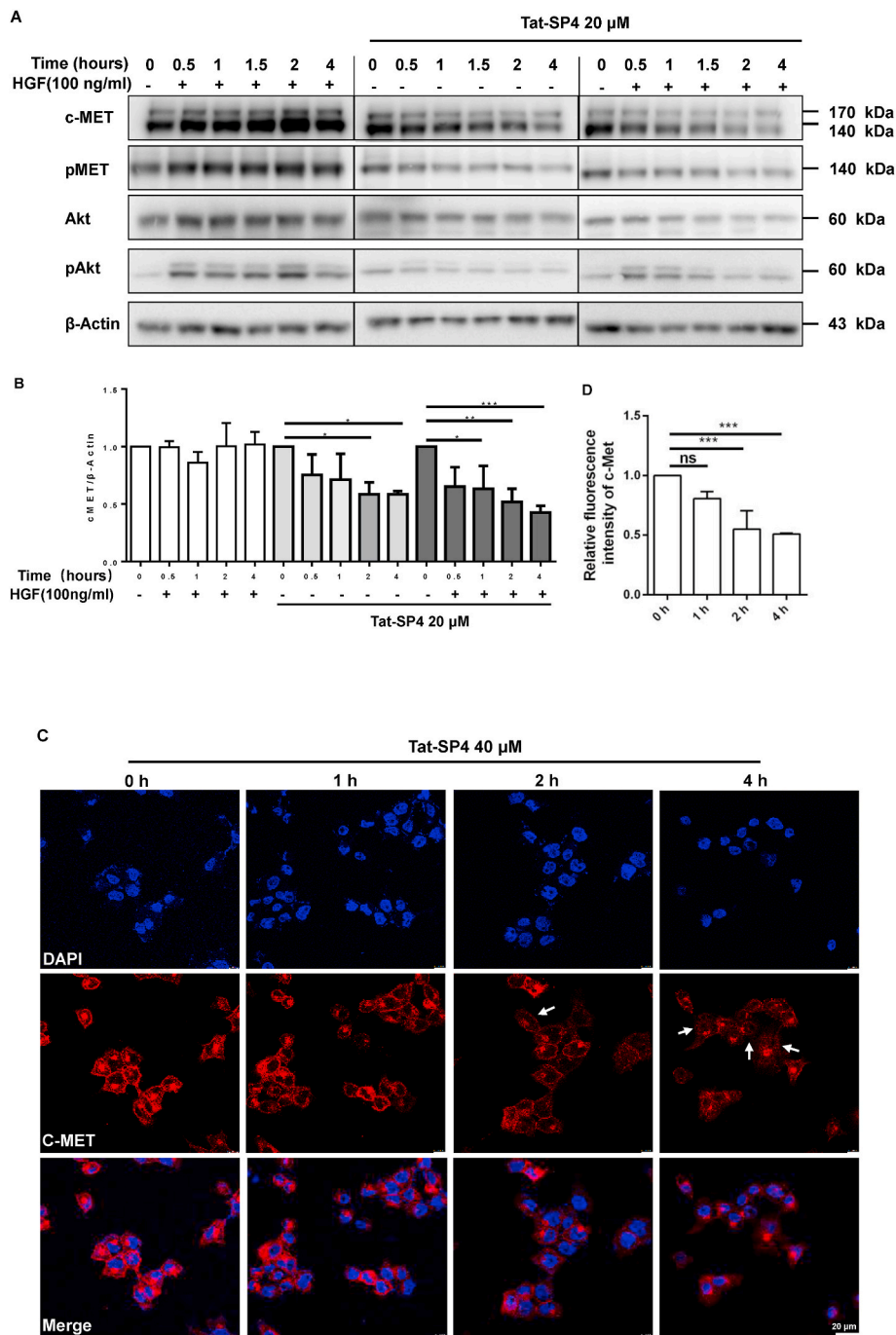


**Fig. 3. Tat-SP4 significantly enhanced endolysosomal degradation of c-MET in HCC cells.** (A) The c-MET level and the downstream oncogenic signaling transduction in MHCC97L cell lysate were analyzed by Western blot at indicated time points after overnight serum-starved (-) and 100 ng/mL HGF treatment (+), Tat-SP4 (20  $\mu$ M) treatment. Blots were probed with anti-c-MET, anti-p-c-MET, anti-Akt, anti-p-Akt and anti- $\beta$ -catenin antibodies. (B). Quantification of the level of c-MET from Western blot data in (A). The individual c-MET levels were normalized to the respective  $\beta$ -Actin in the same blot. Data are presented as mean  $\pm$  SEM (n = 3). \*P < 0.05, \*\*P < 0.05, One-way ANOVA test. (C). Immunofluorescence imaging of c-MET in MHCC97L cells before (0 h) and after treatment with 40  $\mu$ M Tat-SP4 at indicated time points after overnight serum-starved. Cells were blocked and incubated with anti-mouse Alexa Fluor secondary antibodies. Arrows mark those cells with significantly lower level of c-MET after Tat-SP4 treatment. (Scale bar:10  $\mu$ m). (D). Statistical analysis of c-MET fluorescence intensity in (C). The fluorescence intensity at individual time points (1 h, 2 h and 4 h) was normalized to the control at 0 h. Data are presented as mean  $\pm$  SEM (n = 3). \*\*\*P < 0.005, One-way ANOVA test.

signaling pathway.

The impact of Tat-SP4 on endolysosomal degradation of c-MET in MHCC97L cells was further validated by immunofluorescence imaging studies. Our data show that after overnight starvation, c-MET was distributed in two subcellular locations with the population of the mature c-MET spread as a well-defined thin layer on the plasma membrane and the precursor population enriched in Golgi in agreement with previous studies (Fig. 3C) [24]. At 2 h after Tat-SP4 treatment, the population of mature c-MET on the plasma membrane was significantly reduced as shown by its weaker fluorescence intensity while the population of precursor c-MET protein in Golgi was less unaffected (Fig. 3C and D). This difference between the two populations of c-MET supports our western blots results and agrees with previous studies because the mature c-MET on the plasma membrane is believed to undergo active

endolysosomal degradation than the immature c-MET in Golgi.

#### 3.4. Tat-SP4 overrides adaptive resistance to sorafenib in c-MET<sup>+</sup> HCC cells

We used the trypan blue exclusion assay to measure cell viability and to evaluate the anti-proliferative potency of Tat-SP4 in different HCC cells lines. For this study, we also included SNU-449, another HCC cell line with c-MET over-expression. Our results show that for PLC/PRF/5 and Hep3B cells that are c-MET<sup>-</sup> with little to no expression of c-MET, Tat-SP4 exerted minor anti-proliferative effect with IC50 of  $\sim$ 62.08  $\mu$ M and 51.58  $\mu$ M respectively (Fig. 4A & B). However, for the c-MET<sup>+</sup> cell lines MHCC97L and SUN449, Tat-SP4 showed much stronger anti-proliferative effect with IC50 of  $\sim$ 34.17  $\mu$ M and 19.05  $\mu$ M respectively

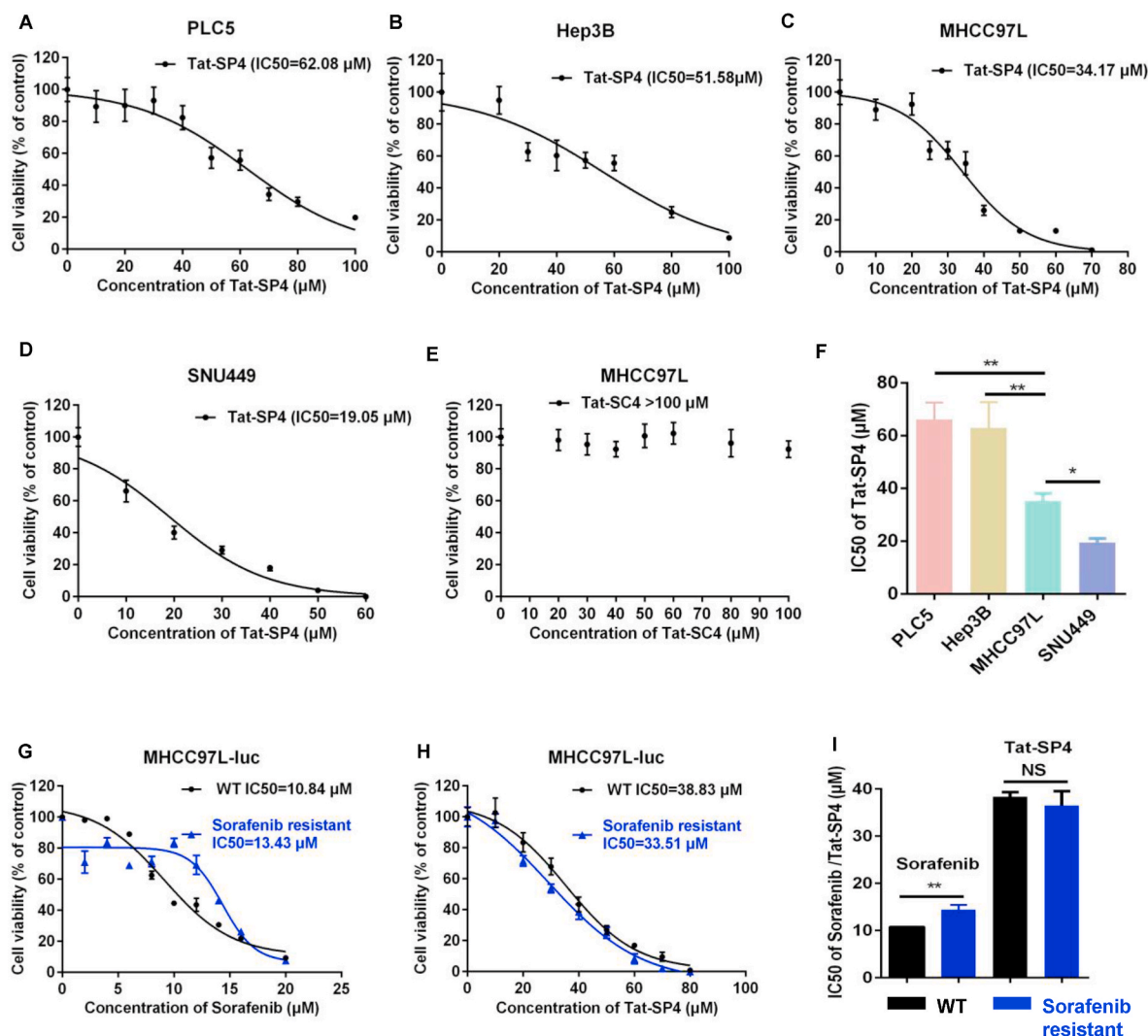


**Fig. 4.** Tat-SP4 shows stronger anti-proliferative effect in cMET<sup>+</sup>HCC cells. (A–D) Cell viability of PLC5, Hep3B, MHCC97L and SNU-499 after treated by different concentrations of Tat-SP4. The estimated IC<sub>50</sub> value is 62.08  $\mu\text{M}$ , 51.58  $\mu\text{M}$ , 34.17  $\mu\text{M}$  and 19.05  $\mu\text{M}$  respectively. (E) Cell viability of MHCC97L after treated by different concentrations of the control peptide Tat-SC4, which contains the scrambled amino acid sequence of Tat-SP4. The estimated IC<sub>50</sub> value is over 100  $\mu\text{M}$ . Data represents mean  $\pm$  SEM of three replicates. (F) Statistical analysis of IC<sub>50</sub> value of PLC5, Hep3B, MHCC97L and SNU-499 as measured in (A–D). Bars represent mean  $\pm$  SEM (n = 3). \*\*P < 0.01; t-test. (G) Cell viability of MHCC97L-luc WT cells and sorafenib resistant MHCC97L-luc cells after treated by different concentrations of sorafenib for 72 h. The estimated IC<sub>50</sub> value is 10.84  $\mu\text{M}$  and 13.43  $\mu\text{M}$ , respectively. (H). MHCC97L-luc WT cells and sorafenib resistant MHCC97L-luc cells treatment with different concentrations of Tat-SP4. The estimated IC<sub>50</sub> value is 38.83  $\mu\text{M}$  and 33.51  $\mu\text{M}$ , respectively. Data represents mean  $\pm$  SEM of three replicates. (I) Statistical analysis of IC<sub>50</sub> value of sorafenib and Tat-SP4 in (G and H). Bars represent mean  $\pm$  SEM (n = 3). \*\*P < 0.01; t-test.

(Fig. 4C & D). In comparison, a control peptide Tat-SC4 with scrambled sequence of Tat-SP4 showed no anti-proliferative effect (Fig. 4E). Notably, the IC<sub>50</sub> values for Tat-SP4 in c-MET<sup>+</sup> HCC cell lines are comparable with those reported for sorafenib as they are all in the  $\mu\text{M}$  range [25]. Thus, the c-MET expression level in HCC cells strongly influences their sensitivity to Tat-SP4 treatment (Fig. 4F).

We also assessed the impact of Tat-SP4 on adaptive resistance to sorafenib in HCC cells. We made use of a previously published MHCC97L-luc cell line that stably over-expresses the luciferase reporter gene and has developed adaptive resistance to sorafenib after being subject to continuous administration of gradually increasing concentrations of sorafenib [22]. While sorafenib inhibited the proliferation of wild-type MHCC97L-luc cells with IC<sub>50</sub> of  $\sim$ 10.84  $\mu\text{M}$ , it inhibited the sorafenib-resistant cells with significantly higher IC<sub>50</sub> of  $\sim$ 13.43  $\mu\text{M}$  (Fig. 4G). This IC<sub>50</sub> difference of  $\sim$ 3  $\mu\text{M}$  is statistically significant, although slightly less than reported in the previous study ( $\sim$ 3.6  $\mu\text{M}$  for wild-type vs.  $\sim$ 10  $\mu\text{M}$  for resistant type) probably due to slight variations in the cell viability protocol [22]. Interestingly, Tat-SP4 inhibited

the proliferation of both wild-type and sorafenib-resistant MHCC97L-luc cells with similar IC<sub>50</sub> of  $\sim$ 38.83 and  $\sim$ 33.51  $\mu\text{M}$  with the small variation not statistically significant (Fig. 4H & I). This is a very exciting finding because it suggests that Tat-SP4 may override adaptive resistance to sorafenib in c-MET<sup>+</sup> HCC cells.

### 3.5. Tat-SP4 triggers predominantly non-apoptotic cell death in c-MET<sup>+</sup> HCC cells

Our previous study reported that Tat-SP4 induced necrotic cell death but not apoptosis in HER2<sup>+</sup> breast cancer cells to exert anti-proliferative effect [15]. As HCC and breast cancer are etiologically distinct, we set out to investigate the type of cell death triggered by Tat-SP4 in c-MET<sup>+</sup> + MHCC97L cells. Flow cytometry experiments with annexin V and propidium iodide (PI) staining were used to differentiate between apoptotic (annexin V positive and PI negative) versus necrotic cell death (positive for both). Our results reveal that Tat-SP4 promptly induced non-apoptotic cell death in dosage-dependent manner (Fig. 5A). Tat-SP4

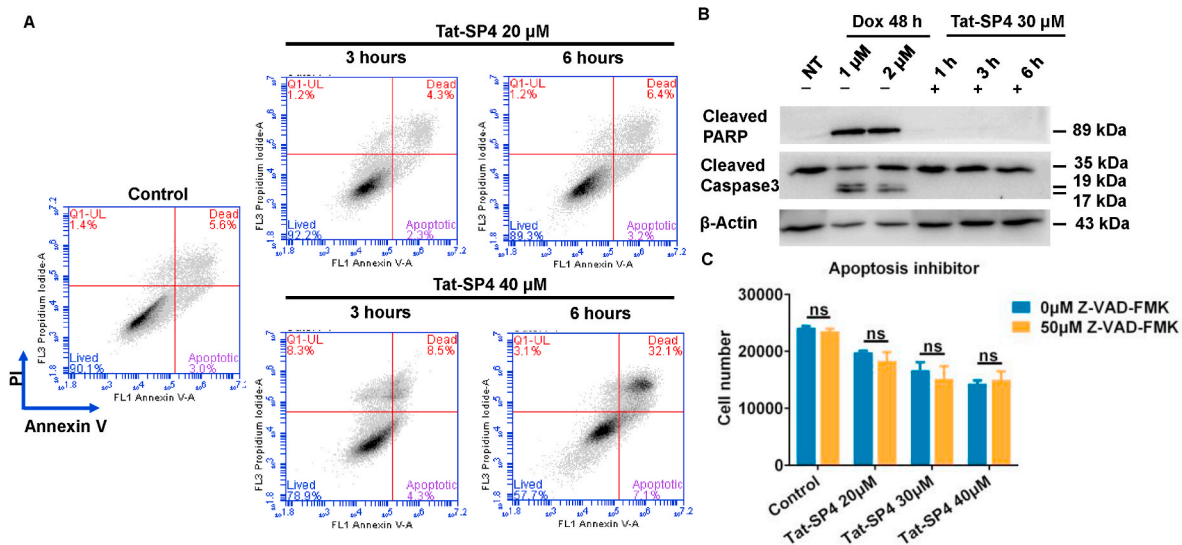


**Fig. 5. Tat-SP4 induces predominantly non-apoptotic cell death in HCC cells.** Flow cytometry analysis with Annexin V/FITC-PI staining was performed in MHCC97L cells after treatment of 40 μM Tat-SP4 for 3 h and 6 h. The percentage of dead cells (PI positive) in Tat-SP4 treatment groups were significantly increased compared with that of control, without notable changes in the population of apoptotic cells. (B) Western blotting of cleaved-PARP and cleaved-Caspase3 in MHCC97L cells treated with either doxorubicin at the specified dosage (1 μM and 2 μM) for 48 h; or with 30 μM Tat-SP4 for different incubation period (1 h, 3 h and 6 h). Doxorubicin induced cleavage of PARP and caspase3 while Tat-SP4 did not. (C) Trypan blue exclusion method to assess the viability of MHCC97L cells treated with Tat-SP4 for 24 h, in the absence or presence of the apoptosis inhibitor Z-VAD-FMK. No rescue effect was observed. Data are presented as mean ± SEM (n = 3). \*\*P < 0.01, unpaired *t*-test. (For interpretation of the references to color in this figure legend, the reader is referred to the Web version of this article.)

treatment at 20 μM didn't induce significant cell death as the amount of apoptotic and dead cells was similar to that of the control sample without any treatment (Fig. 5A). After Tat-SP4 treatment at 40 μM, 8.5% of MHCC97L cells underwent necrotic cell death at 2 h and this number quadrupled to 32.1% at 4 h (Fig. 5A). This quick progress further suggests that MHCC97L cells underwent non-apoptotic cell death as apoptosis is known to proceed in an orderly and controlled manner over longer time period [26]. In comparison, the level of apoptosis did rise from 4.3% to 7.1%, but this change is only one tenth of the rise in necrotic cell death (Fig. 5A).

To further investigate the involvement of apoptosis in Tat-SP4 induced cell death, we assessed the cleavage of PARP and caspase-3, two signature events for apoptosis. Doxorubicin, a chemo drug known to induce apoptosis, led to cleavage of both proteins in MHCC97L cells while Tat-SP4 did not (Fig. 5B). Additionally, Z-VAD-FMK, an apoptosis inhibitor, did not rescue cell death caused by Tat-SP4 (Fig. 5C). Thus, Tat-SP4 induced non-apoptotic cell death in HCC cells similar to what we reported in HER2+ breast cancer cells [15]. This mechanism is in distinct contrast to the apoptosis induced by sorafenib in HCC cells [27].

#### 4. Discussion

Growth factor signaling pathways mediated by receptor tyrosine kinases like EGFR, VEGFR, FGFR, PDGFR and c-MET drive many fundamental cellular processes such as proliferation, differentiation and survival [28]. Abnormal activation of these kinases, often through gene amplification and somatic mutations, has causal effect on multiple human cancers including NSCLC, breast cancer and colorectal cancer [28]. Consequently, these kinases have become the most extensively explored targets for cancer drug discovery. Inhibitors of these kinases such as TKIs and mAbs have achieved impressive clinical success with gefitinib for NSCLC and trastuzumab for breast cancer as notable examples.

However, this strategy only generated limited success for HCC. Sorafenib was the first TKI approved for HCC and has been used as the major first-line treatment since 2008 [4]. However, it only offered modest survival benefit of about 3 months compared to placebo and

patients readily developed resistance in the course of treatment [4,29]. Lenvatinib showed similar clinical benefit as sorafenib and was approved in 2018 on grounds of being non-inferior [5]. Regorafenib and cabozantinib are newer TKIs approved as second-line treatments for HCC patients who have progressed after sorafenib treatment, but they only brought survival benefit of about 2 months as well [6,7].

c-MET has remained an important drug target for HCC as its over-expression and mutations have been found to correlate with poor prognosis [16,30,31]. Unfortunately, TKIs and mAbs that inhibit c-MET at either its intracellular kinase domain or its extracellular ligand binding domain failed to show clinical benefits [16,30,31]. One possible reason is the extensive crosstalk between c-MET and other oncogenic signaling pathways such as those driven by EGFR, VEGFR and Wnt may help to overcome the inhibitory effect exerted by TKIs and mAbs on the kinase domain alone [16,30,31].

Here we present a novel approach to inhibit c-MET by targeting the autophagy process. Our autophagy-inducing peptide Tat-SP4 triggered significant autophagic response in multiple HCC cell lines regardless of their genetic background. Tat-SP4 also promoted the endolysosomal degradation of c-MET, which led to reduced phosphorylation of c-MET and downstream targets like Akt to attenuate the HGF/c-MET signaling pathway. Compared to TKIs like sorafenib, Tat-SP4 inhibits c-MET through the unique mechanism of degrading the entire protein rather than just inhibiting the kinase domain. Such degradation may be advantageous as it could also remove the crosstalk between c-MET and other oncogenic receptors, thus leading to broader inhibitory effect on the entire growth signaling network in HCC cells. Indeed, the anti-proliferative efficacy of Tat-SP4, with IC<sub>50</sub> values in the ~30–50 μM range, is comparable to other autophagy modulators such as CQ, thus validating our targeting strategy [32].

Intriguingly, Tat-SP4 showed little effect on enhancing the endolysosomal degradation of EGFR in HCC cells, although it did exert such effect in NSCLC and breast cancer cells [14,15]. Beclin 1 has been reported to associate with early endosomes and promote their maturation and trafficking to lysosomes [33]. Thus Beclin 1, as well as our Beclin 1-targeting stapled peptides including Tat-SP4, may be particularly effective in promoting the endolysosomal degradation of molecules that



are captured in endosomes with slow maturation rate. One particular feature we noted in HCC cells is the rapid turnover of endogenous EGFR, which may leave little room for further enhancement by Tat-SP4.

Most excitingly, Tat-SP4 shows the potential in overriding adaptive resistance to sorafenib in c-MET<sup>+</sup> HCC cells. Tat-SP4 exerted potent anti-proliferative effect in c-MET<sup>+</sup> HCC cells with IC<sub>50</sub> comparable to sorafenib. It also showed similar IC<sub>50</sub> values for both wild-type and sorafenib-resistant c-MET<sup>+</sup> HCC cells. Notably, over-expression of receptor tyrosine kinases including EGFR, FGFR, PDGFR and c-MET has been shown to drive sorafenib resistances [22]. In this regard, Tat-SP4 can be particularly effective in terms of overriding sorafenib resistance as our data shows that it can promote the endolysosomal degradation of these kinases in bulk. It is possible HCC cells may eventually acquire resistance to Beclin 1-targeting modalities like Tat-SP4 through possible means of genetic alteration and metabolic reprogramming. But with its distinct mechanism, Tat-SP4 may serve as a novel therapeutic agent that complement and synergize with sorafenib to enhance its clinical efficacy.

#### Author contributions

SG, NL, XZ and JY carried out the molecular and cellular assays. SG wrote sections of the manuscript. YZ supervised the project, designed the experiments, analyzed the data and completed the manuscript. All authors have given approval to the final version of the manuscript.

#### Conflict of interest statement

The authors have filed patent applications in U.S. and China based on this work.

#### Declaration of competing interest

The authors have filed patent applications in U.S. and China based on this work.

The authors declare no other forms of financial interest.

#### Data availability

Data will be made available on request.

#### Acknowledgment

The work was supported by grants from the Research Grants Council of Hong Kong (N-PolyU503/16, PolyU 151062/18 M, 15103819, 15106421, R5050-18, and AoE/M-09/12), the Health and Medical Research Fund of Hong Kong (HMRFO8191866), the Innovation and Technology Fund of Hong Kong (MRP/043/21), Shenzhen Basic Research Program of China (JCYJ20170818104619974, JCYJ20210324133803009) and Hong Kong Polytechnic University to YZ. All authors have given approval to the final version of the manuscript. The authors declare no competing financial interests. All authors have given approval to the final version of the manuscript.

#### Appendix A. Supplementary data

Supplementary data to this article can be found online at <https://doi.org/10.1016/j.bbrep.2022.101412>.

#### References

- [1] H. Sung, J. Ferlay, R.L. Siegel, M. Laversanne, I. Soerjomataram, A. Jemal, F. Bray, Global cancer statistics 2020: GLOBOCAN estimates of incidence and mortality worldwide for 36 cancers in 185 countries, *Ca - Cancer J. Clin.* 71 (2021) 209–249.
- [2] A. Forner, M. Reig, J. Bruix, Hepatocellular carcinoma, *Lancet* 391 (2018) 1301–1314.
- [3] J.M. Llovet, R.K. Kelley, A. Villanueva, A.G. Singal, E. Pikarsky, S. Roayaie, R. Lencioni, K. Koike, J. Zucman-Rossi, R.S. Finn, Hepatocellular carcinoma, *Nat. Rev. Dis. Prim.* 7 (2021) 6.
- [4] J.M. Llovet, S. Ricci, V. Mazzaferro, P. Hilgard, E. Gane, J.F. Blanc, A.C. de Oliveira, A. Santoro, J.L. Raoul, A. Forner, M. Schwartz, C. Porta, S. Zeuzem, L. Bolondi, T.F. Greten, P.R. Galle, J.F. Seitz, I. Borbath, D. Haussinger, T. Giannaris, M. Shan, M. Moscovici, D. Voliotis, J. Bruix, S.I.S. Group, Sorafenib in advanced hepatocellular carcinoma, *N. Engl. J. Med.* 359 (2008) 378–390.
- [5] M. Kudo, R.S. Finn, S. Qin, K.H. Han, K. Ikeda, F. Piscaglia, A. Baron, J.W. Park, G. Han, J. Jassem, J.F. Blanc, A. Vogel, D. Komov, T.R.J. Evans, C. Lopez, C. Dutcus, M. Guo, K. Saito, S. Kraljevic, T. Tamai, M. Ren, A.L. Cheng, Lenvatinib versus sorafenib in first-line treatment of patients with unresectable hepatocellular carcinoma: a randomised phase 3 non-inferiority trial, *Lancet* 391 (2018) 1163–1173.
- [6] J. Bruix, S. Qin, P. Merle, A. Granito, Y.H. Huang, G. Bodoky, M. Pracht, O. Yokosuka, O. Rosmorduc, V. Breder, R. Gerolami, G. Masi, P.J. Ross, T. Song, J. P. Bronowicki, I. Ollivier-Hourmand, M. Kudo, A.L. Cheng, J.M. Llovet, R.S. Finn, M.A. LeBerre, A. Baumhauer, G. Meinhardt, G. Han, R. Investigators, Regorafenib for patients with hepatocellular carcinoma who progressed on sorafenib treatment (RESORCE): a randomised, double-blind, placebo-controlled, phase 3 trial, *Lancet* 389 (2017) 56–66.
- [7] G.K. Abou-Alfa, T. Meyer, A.L. Cheng, A.B. El-Khoueiry, L. Rimassa, B.Y. Ryoo, I. Cicin, P. Merle, Y. Chen, J.W. Park, J.F. Blanc, L. Bolondi, H.J. Klumpen, S. L. Chan, V. Zagonel, T. Pressiani, M.H. Ryu, A.P. Venook, C. Hessel, A.E. Borgman-Hagey, G. Schwab, R.K. Kelley, Cabozantinib in patients with advanced and progressing hepatocellular carcinoma, *N. Engl. J. Med.* 379 (2018) 54–63.
- [8] R.S. Finn, S. Qin, M. Ikeda, P.R. Galle, M. Ducreux, T.Y. Kim, M. Kudo, V. Breder, P. Merle, A.O. Kaseb, D. Li, W. Verret, D.Z. Xu, S. Hernandez, J. Liu, C. Huang, S. Mulla, Y. Wang, H.Y. Lim, A.X. Zhu, A.L. Cheng, I.M. Investigators, Atezolizumab plus bevacizumab in unresectable hepatocellular carcinoma, *N. Engl. J. Med.* 382 (2020) 1894–1905.
- [9] A.X. Zhu, Y.K. Kang, C.J. Yen, R.S. Finn, P.R. Galle, J.M. Llovet, E. Assenat, G. Brandi, M. Pracht, H.Y. Lim, K.M. Rau, K. Motomura, I. Ohno, P. Merle, B. Daniele, D.B. Shin, G. Gerken, C. Borg, J.B. Hiriart, T. Okusaka, M. Morimoto, Y. Hsu, P.B. Abada, M. Kudo, R.-s. investigators, Ramucirumab after sorafenib in patients with advanced hepatocellular carcinoma and increased alpha-fetoprotein concentrations (REACH-2): a randomised, double-blind, placebo-controlled, phase 3 trial, *Lancet Oncol.* 20 (2019) 282–296.
- [10] B. Levine, G. Kroemer, Biological functions of autophagy genes: a disease perspective, *Cell* 176 (2019) 11–42.
- [11] N. Mizushima, B. Levine, Autophagy in human diseases, *N. Engl. J. Med.* 383 (2020) 1564–1576.
- [12] Z. Yang, D.J. Klionsky, Mammalian autophagy: core molecular machinery and signaling regulation, *Curr. Opin. Cell Biol.* 22 (2010) 124–131.
- [13] J. Cui, Z. Gong, H.M. Shen, The role of autophagy in liver cancer: molecular mechanisms and potential therapeutic targets, *Biochim. Biophys. Acta* 1836 (2013) 15–26.
- [14] S. Wu, Y. He, X. Qiu, W. Yang, W. Liu, X. Li, Y. Li, H.M. Shen, R. Wang, Z. Yue, Y. Zhao, Targeting the potent Beclin 1-UVRAG coiled-coil interaction with designed peptides enhances autophagy and endolysosomal trafficking, *Proc. Natl. Acad. Sci. U. S. A.* 115 (2018) E5669–E5678.
- [15] Q. Yang, X. Qiu, X. Zhang, Y. Yu, N. Li, X. Wei, G. Feng, Y. Li, Y. Zhao, R. Wang, Optimization of Beclin 1-targeting stapled peptides by staple scanning leads to enhanced antiproliferative potency in cancer cells, *J. Med. Chem.* 64 (2021) 13475–13486.
- [16] S. Giordano, A. Columbano, Met as a therapeutic target in HCC: facts and hopes, *J. Hepatol.* 60 (2014) 442–452.
- [17] L.L. Rojas-Puentes, M. Gonzalez-Pinedo, A. Crismatt, A. Ortega-Gomez, C. Gamboa-Vignolle, R. Nunez-Gomez, Y. Dorantes-Gallaretta, C. Arce-Salinas, O. Arrieta, Phase II randomized, double-blind, placebo-controlled study of whole-brain irradiation with concomitant chloroquine for brain metastases, *Radiat. Oncol.* 8 (2013) 209.
- [18] J. Chen, X. Zhang, S. Gao, N. Li, V. Keng, Y. Zhao, A Beclin 1-targeting stapled peptide synergizes with erlotinib to potently inhibit proliferation of non-small-cell lung cancer cells, *Biochem. Biophys. Res. Commun.* 636 (2022) 125–131.
- [19] K. Adibkia, A. Ehsani, A. Jodaee, E. Fathi, R. Farahzadi, M. Barzegar-Jalali, Silver nanoparticles induce the cardiomyogenic differentiation of bone marrow derived mesenchymal stem cells via telomere length extension, *Beilstein J. Nanotechnol.* 12 (2021) 786–797.
- [20] E. Fathi, S.A. Mesbah-Namin, I. Viotor, R. Farahzadi, Mesenchymal stem cells cause induction of granulocyte differentiation of rat bone marrow C-kit(+) hematopoietic stem cells through JAK3/STAT3, ERK, and PI3K signaling pathways, *Iranian journal of basic medical sciences* 25 (2022) 1222–1227.
- [21] E. Fathi, S. Vandghanooni, S. Montazersaheb, R. Farahzadi, Mesenchymal stem cells promote caspase-3 expression of SH-SY5Y neuroblastoma cells via reducing telomerase activity and telomere length, *Iranian journal of basic medical sciences* 24 (2021) 1583–1589.
- [22] C.O.N. Leung, M. Tong, K.P.S. Chung, L. Zhou, N. Che, K.H. Tang, J. Ding, E.Y. T. Lau, I.O.L. Ng, S. Ma, T.K.W. Lee, Overriding Adaptive Resistance to Sorafenib through Combination Therapy with Src Homology 2 Domain-Containing Phosphatase 2 Blockade in Hepatocellular Carcinoma, *vol. 72, 2020*, pp. 155–168.
- [23] T. Shibata, H. Aburatani, Exploration of liver cancer genomes, *Nat. Rev. Gastroenterol. Hepatol.* 11 (2014) 340–349.
- [24] N.M. Frazier, T. Brand, J.D. Gordon, J. Grandis, N. Jura, Overexpression-mediated activation of MET in the Golgi promotes HER3/ERBB3 phosphorylation, *Oncogene* 38 (2019) 1936–1950.



- [25] Q. Wang, C. Bin, Q. Xue, Q. Gao, A. Huang, K. Wang, N. Tang, GSTZ1 sensitizes hepatocellular carcinoma cells to sorafenib-induced ferroptosis via inhibition of NRF2/GPX4 axis, *Cell Death Dis.* 12 (2021) 426.
- [26] R.C. Taylor, S.P. Cullen, S.J. Martin, Apoptosis: controlled demolition at the cellular level, *Nat. Rev. Mol. Cell Biol.* 9 (2008) 231–241.
- [27] X. Zhao, C. Tian, W.M. Puszyk, O.O. Ogunwobi, M. Cao, T. Wang, R. Cabrera, D. R. Nelson, C. Liu, OPA1 downregulation is involved in sorafenib-induced apoptosis in hepatocellular carcinoma, *Laboratory investigation; a journal of technical methods and pathology* 93 (2013) 8–19.
- [28] A. Gschwind, O.M. Fischer, A. Ullrich, The discovery of receptor tyrosine kinases: targets for cancer therapy, *Nat. Rev. Cancer* 4 (2004) 361–370.
- [29] J. Chen, D.G. Duda, Overcoming sorafenib treatment-resistance in hepatocellular carcinoma: a future perspective at a time of rapidly changing treatment paradigms, *EBioMedicine* 52 (2020), 102644.
- [30] R. Guo, J. Luo, J. Chang, N. Rekhtman, M. Arcila, A. Drilon, MET-dependent solid tumours - molecular diagnosis and targeted therapy, *Nat. Rev. Clin. Oncol.* 17 (2020) 569–587.
- [31] E. Gherardi, W. Birchmeier, C. Birchmeier, G. Vande Woude, Targeting MET in cancer: rationale and progress, *Nat. Rev. Cancer* 12 (2012) 89–103.
- [32] T. Hu, P. Li, Z. Luo, X. Chen, J. Zhang, C. Wang, P. Chen, Z. Dong, Chloroquine inhibits hepatocellular carcinoma cell growth in vitro and in vivo, *Oncol. Rep.* 35 (2016) 43–49.
- [33] N.C. McKnight, Y. Zhong, M.S. Wold, S. Gong, G.R. Phillips, Z. Dou, Y. Zhao, N. Heintz, W.X. Zong, Z. Yue, Beclin 1 is required for neuron viability and regulates endosome pathways via the UVRAG-VPS34 complex, *PLoS Genet.* 10 (2014), e1004626.